Available online at www.sciencedirect.com
ScienceDirect
International Journal of Heat and Mass Transfer 50 (2007) 4219–4228
International Journal of HEAT and MASS TRANSFER
www.elsevier.com/locate/ijhmt

Subsonic compressible flow in two-sided lid-driven cavity. Part II: Unequal walls temperatures

P. Shah [a], B. Rovagnati [a], F. Mashayek [a,*], G.B. Jacobs [b]

[a] Department of Mechanical and Industrial Engineering, University of Illinois at Chicago, 842 West Taylor Street, Chicago, IL 60607, United States
[b] Department of Aerospace Engineering and Engineering Mechanics, San Diego State University, San Diego, CA 92182, United States

Received 2 January 2007; received in revised form 16 February 2007
Available online 3 May 2007

Abstract

This paper studies the effect of unequal walls temperatures for a two-dimensional, two-sided, lid-driven cavity via numerical simulations using a multi-domain, spectral element method. The flow is driven by steadily moving the two opposite walls vertically in opposite directions. Different temperatures are applied on the two moving walls and the effect of the resulting heat transfer on the two-dimensional flow is studied. An analysis of the flow evolution shows that, with increasing the temperature difference between the opposite moving walls, the steady state flow changes from a single-vortex to a two-vortex pattern. Energy balance studies are conducted at steady state and during flow evolution. The evolution and distribution of heat transfer at all walls and work done at the moving walls are studied.

1. Introduction

The fluid motion in rectangular enclosures has been of fundamental concentration because of its significance to basic and engineering applications, e.g., coating and drying technologies, flow over structures in airfoils or cooling flow over electronic devices. In Part I [1] of this study, we considered the flow inside a two-sided, lid-driven cavity when all walls were at the same temperature. In this paper, the effect of unequal walls temperatures is studied by numerical simulations using a multi-domain, spectral element method. The flow is driven by steadily moving the two opposite walls vertically in opposite directions, and is differentially heated by imposing unequal temperatures at these moving boundaries.

A brief review of the extensively studied lid-driven cavity problem was reported in Part I [1]. In contrast to other works found in literature, in Part I the compressibility effects were accounted for and the evolution of the flow was studied for a variety of cases. The effect of the cavity aspect ratio, the Reynolds number and the Mach number on the flow were investigated. It was found that at lower Reynolds numbers, the flow pattern consisted of two separate co-rotating vortices contiguous to the moving walls. For higher Reynolds numbers, the initially two-vortex flow turned into a single elliptical vortex occupying most of the cavity. For a higher aspect ratio, the flow patterns were dissimilar in that the streamlines became more and more elliptic. For aspect ratios as high as 2.5, at high Reynolds numbers, a three-vortex stage was formed. It was also found that the compressibility effects are not very significant for Mach numbers less than 0.4. Dissipation of kinetic energy into internal energy changed the temperature field especially near the boundaries.

Here, we further investigate the lid-driven cavity problem, by considering the temperature boundary conditions to be different on the two moving walls, as it is required in applications such as drying processes. When the lid-driven sides are differentially heated, the temperature gradient in the cavity generates forces due to density variation which, together with the forced convection due to shear, result in a mixed convection heat transfer. A numerical investigation of this phenomenon was conducted in [2], where the

* Corresponding author. Tel.: +1 312 996 1154; fax: +1 312 413 0447.
E-mail address: mashayek@uic.edu (F. Mashayek).

0017-9310/$ - see front matter © 2007 Elsevier Ltd. All rights reserved.
doi:10.1016/j.ijheatmasstransfer.2007.02.029

Nomenclature

c_p	constant pressure specific heat of the fluid
L	length
L_f	reference length
$L_{w,left}$	length of the left wall
$L_{w,right}$	length of the right wall
L_h	length of the horizontal walls
L_v	length of the vertical walls
M_f	$U_f^*/\sqrt{\gamma R^* T_f^*}$ reference Mach number
Ma	$uM_f/\sqrt{T}$ Mach number
Pr	$c_p^*\mu^*/\kappa^*$ Prandtl number
$Q_{net,bottom}$	the net heat transfer at the bottom wall
$Q_{net,top}$	the net heat transfer at the top wall
$Q_{net,left}$	the net heat transfer at the left wall
$Q_{net,right}$	the net heat transfer at the right wall
$W_{net,left}$	the net work done at the left wall
$W_{net,right}$	the net work done at the right wall
Q_{net}	the net heat transfer at all the four walls
W_{net}	the net work done at the moving walls
R	gas constant
Re	$\rho^* U^* L^*/\mu^*$ Reynolds number
t	time
T	temperature
T_i	initial temperature
T_f	reference temperature
$T_{w,left}$	temperature of the left wall
$T_{w,right}$	temperature of the right wall
u, v	velocity of the fluid in x- and y-directions respectively
V_{wall}	wall velocity
$V_{w,left}$	velocity of the left wall
$V_{w,right}$	velocity of the right wall
U_f	reference velocity
x, y	spatial coordinates
w	depth of the cavity in z-direction

Greek symbols

γ	ratio of the specific heats of the fluid
Γ	aspect ratio of the cavity
κ	thermal conductivity
μ	dynamic viscosity
ρ	density

Subscripts

i	initial
f	reference variable

Superscript

$*$	physical space variable

mechanism of aiding and opposing forces in shear and buoyancy driven cavity was studied. We refer to Ref. [3] and references therein for a brief overview of this kind of problem. The focus of the work in Ref. [3] was to study the effect of radiation on the mixed convection as generated by buoyancy-opposing flow and buoyancy-aiding flow.

As observed in Ref. [1], viscous heating plays an important role in the dynamics of fluids with strongly temperature-dependent density because of the coupling between the energy and momentum equations. When the temperature gradients induced by viscous heating are very pronounced, local instabilities may occur and the triggering of secondary flows is possible. Therefore, unequal wall temperatures is expected to strengthen such effect. The latter and other aspects of the evolution of the flow will be studied in this work. The present paper is organized as follows. In the next section, the problem formulation is presented. Section 2 is dedicated to discussions of the numerical results. Finally, concluding remarks are provided in Section 3.

2. Problem description

In a similar manner as in Part I [1], we consider the two-dimensional, two-sided lid-driven cavity flow with initially uniform temperature T_i and all the four surrounding walls at rest as shown in Fig. 1. The two moving walls are referred to as the left and the right moving walls for conve-

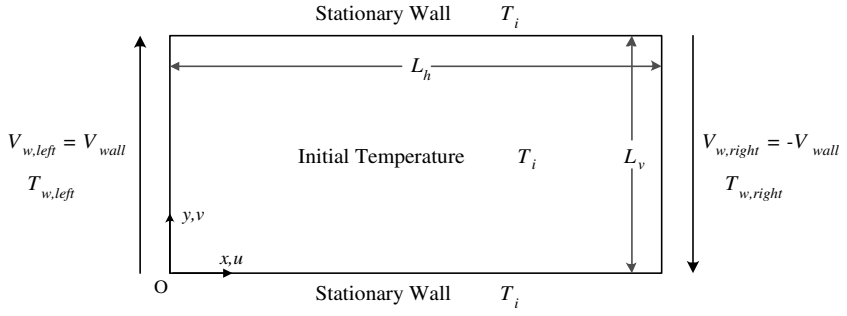

Fig. 1. Schematic diagram of the two-sided lid-driven cavity.

nience and the temperatures on the two walls as $T_{w,left}$ and $T_{w,right}$, respectively. The velocity boundary conditions are employed on the two vertical walls, by giving them the same magnitude of velocity V_{wall}, but in opposite directions in order to have anti-parallel wall motion, i.e. $V_{w,right} = -V_{wall}$ and $V_{w,left} = V_{wall}$. The u velocity component for the moving walls is zero. A Reynolds number of 700, a Mach number of 0.4, and an aspect ratio of 1.955 are chosen for this study.

We refer to Refs. [1,4] for the description of the governing (Navier–Stokes) equations of the cavity problem. The numerical solution of the governing equations is achieved by use of a multi-domain, staggered-grid, Chebyshev, spectral element code. Details of the code were reported elsewhere [5–7]. Validation and resolution study for the case of equal walls temperatures were presented in Refs. [1,4]. The same mesh with 80 elements clustered near the boundaries is used for this study. However, it is observed that a polynomial order of 6, which was sufficient for resolving the flow fields for equal wall temperatures, is not sufficient for the present study. Thus, a grid with polynomial order of 8 is used.

3. Results

The previous work (Ref. [1]) dealt with the case wherein, the moving wall temperatures are equal to the initial temperature, i.e. $T_{w,right} = T_{w,left} = T_i$. We refer to this as case I, and compare the cases with unequal temperature boundary conditions to this case. Unequal temperature boundary conditions are employed on the two vertical moving walls by increasing the temperature of one moving wall and decreasing the temperature of another moving wall, relative to the initial temperature, as listed in Table 1 for cases II–VI. For example, in case II, $T_{w,right} = 1.05T_i$ and $T_{w,left} = 0.95T_i$. Thus, there is a $\pm 5\%$ difference in the temperatures of the moving walls from the initial condition. Cases II–VI have increasing percentage difference between the initial condition of temperature and the temperatures of the moving walls. The temperatures of the stationary walls remain equal to the initial temperatures for all the cases.

3.1. Flow evolution

When the vertical walls are not only given velocity but also different temperatures, i.e. cases II–VI, interesting flow changes take place. Such a difference in the temperatures of the two moving walls from the initial temperature and from each other, gives rise to large temperature gradients in the area near the moving walls. This changes the temperature profiles, and therefore, the velocity profiles change in the cavity. When the temperature gradients in the domain are very pronounced, local instabilities may occur and the triggering of secondary flows is potential [8]. The flow patterns obtained for cases II–VI are compared with the flow patterns obtained by a simulation for case I. Various stages of flow development are illustrated in Fig. 2 for cases I–VI. The streamlines are colored by temperature. The flow stages appearing before 30 time units show some similarity for cases I–IV. (The temperature fields, however, have obvious differences.) Because these flow stages have been discussed in detail in Part I [1], they are not included in Fig. 2.

Table 1
Case studies for unequal temperature boundary conditions, $T_i = 6.25$ and $Ma = 0.4$

Case	Percentage difference from T_i (%)	$T_{w,left}$	$T_{w,right}$	$T_{w,top} = T_{w,bottom}$
I	±0	$1.0T_i$	$1.0T_i$	T_i
II	±5	$0.95T_i$	$1.05T_i$	T_i
III	±10	$0.9T_i$	$1.1T_i$	T_i
IV	±20	$0.8T_i$	$1.2T_i$	T_i
V	±30	$0.7T_i$	$1.3T_i$	T_i
VI	±40	$0.6T_i$	$1.4T_i$	T_i

For case I, $T_{w,left} = T_i$, while for the other cases, $T_{w,left} < T_i$. On the other hand, $T_{w,right} = T_i$ for case I and $T_{w,right} > T_i$ for the other cases. On the higher temperature side of cases II–VI, the ideal gas has a lower density, and vice versa on the lower temperature side. For example, for case IV near the right moving wall, the density is 0.85 and near the left moving wall, the density is close to 1.15, while for case I, the density is close to 1.01 near both walls. Because of a lower density on the higher temperature (i.e. the right) side, the fluid has less inertia on this side. This results in asymmetrical flow states. As the two smaller vortices, move towards the moving walls, it is easier for the upper (small) vortex to push the lower density fluid at its right compared to the lower vortex to push the high density fluid at its left. Therefore, the upper vortex increases in size as it moves towards its right, pushing the right vortex to decrease in size and making space for its own growth. Meanwhile, the lower vortex is not able to push the high density fluid at its left and therefore, decreases in size. Due to the tendency of vortices to remain circular, the two larger vortices (the right one of which has decreased in size by now), try to merge. The combination of the two vortices into a single vortex is harder for unequal wall temperatures as compared to case I with equal wall temperatures. The two vortices appear partially merged in cases II–IV, but are not in a merged stage for cases V and VI at steady state.

For case V, that is for ±30% difference in the initial and the moving wall temperatures, similar stages to those appearing for cases II–IV take place. However, because of a higher temperature gradient, the flow pattern obtained is not stable in case V. Also, the density of the hot vortex on the right side is so low, that the upper right vortex is able to push its way through the partially merged two vortices (see Fig. 2 for case V at $t = 45$). At steady state, the unstable smaller vortex in the upper (hot) right corner, is able to merge with the other smaller vortex which is situated at the bottom center of the cavity. Such a flow stage at steady state was observed for $Re = 700$ at $\Gamma = 2.0$ with no difference between the initial and boundary temperatures.

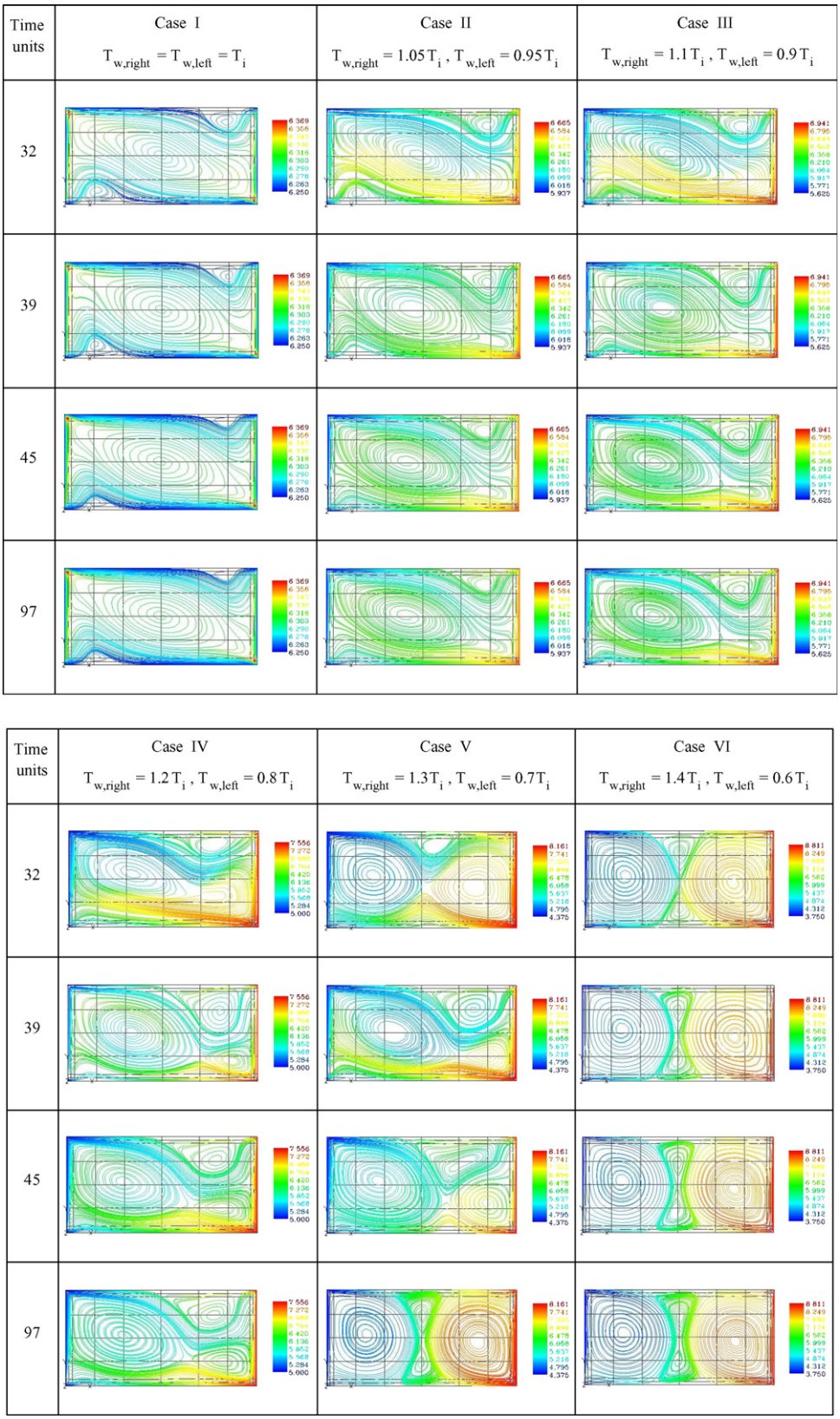

Fig. 2. Flow stages for cases I–VI. The streamlines are colored by temperature. The color bar next to each figure shows the temperature distribution in the domain. (For interpretation of the references in color in this figure legend, the reader is referred to the web version of this article.)

For case VI, the flow stages seen for cases I–V never occur. Though the final flow pattern at steady state for cases V and VI are similar, flow evolution with time is different. Case VI has a temperature difference of 80%

between the two moving walls. This asymmetry in temperature leads to large asymmetry in density and makes it harder for the two vortices to combine. The large (hot) right vortex formed initially rotates with a high velocity (because of low inertia) and there is not enough time for these two vortices to push the fluid between them away in order to combine. Moreover, the coupled effect of the moving walls is not strong enough compared to the effect of the high temperature gradient. The center vortices, therefore, instead of shifting towards the trailing edges of the moving walls, can combine with each other. The two smaller vortices in the center combine owing to the inherent tendency of these vortices to remain circular. Therefore, the steady state for case VI is a two-vortex stage with the smaller vortices in the center partially merged. Though the vortex on the left has a very high inertia, it does not grow beyond this limit because of its tendency to stay circular and because of the high vorticity of the vortices in the center.

The case with 40% difference in the temperature of the moving walls and the initial temperature and $\Gamma = 1.955$ (i.e. case VI) can be compared to the case with same initial temperature and temperature of the walls and $\Gamma = 2.0$. The comparison suggests that the flow evolution and steady state flow topologies are similar for both cases. The flow in a cavity with low aspect ratio, with unequal temperatures at the moving walls, behaves like the flow in a cavity with high aspect ratio, and same temperatures of the moving walls. This shows that temperature gradient has a stabilizing effect on the flow.

3.2. Energy balance

The cavity under consideration is a closed system where no material is transferred across its boundaries. Only heat and work are transferred to/from the system. The difference between the heat transfer by the system and the work done on the system, is the rate of change of energy in the closed system. At steady state, the net energy in the closed system does not change. In this section, we explore the energy balance of the system in cases I–VI.

By convention, work done on the system is negative and work done by the system is positive. Also, heat transfer from the system is negative and heat transfer to the system is positive. In dimensional form, the heat transfer and work through the left wall, for example, are respectively calculated from

$$Q^*_{\text{net,left}} = -\int_0^{L_{\text{w,left}}} \kappa^* \frac{\partial T^*}{\partial x^*} w^* \, \mathrm{d}y^*,$$
$$W^*_{\text{net,left}} = \int_0^{L_{\text{w,left}}} \mu^* \frac{\partial v^*}{\partial x^*} w^* \, \mathrm{d}y^* V^*_{\text{w,left}}, \tag{1}$$

where the subscript * shows a dimensional variable and w^* is the depth of the cavity. Heat transfer and work through other walls are defined analogously. There is no work done by the fixed walls since their velocities are zero. The net heat transfer and work for the entire cavity are, thus, described in non-dimensional form as

$$\begin{aligned} Q_{\text{net}} &= Q_{\text{net,bottom}} + Q_{\text{net,top}} + Q_{\text{net,left}} + Q_{\text{net,right}} \\ &= -\int_0^{\Gamma} \left[\frac{\partial T}{\partial y}\right]_{\text{bottom}} \mathrm{d}x - \int_0^{\Gamma} \left[\frac{\partial T}{\partial y}\right]_{\text{top}} \mathrm{d}x \\ &\quad - \int_0^{1} \left[\frac{\partial T}{\partial x}\right]_{\text{left}} \mathrm{d}y - \int_0^{1} \left[\frac{\partial T}{\partial x}\right]_{\text{right}} \mathrm{d}y, \end{aligned} \tag{2}$$

$$\begin{aligned} W_{\text{net}} &= W_{\text{net,left}} + W_{\text{net,right}} \\ &= (\gamma - 1) Pr M_{\text{f}}^2 \left\{ \int_0^{1} \left[\frac{\partial v}{\partial x}\right]_{\text{left}} \mathrm{d}y \, V_{\text{w,left}} \cdot \right. \\ &\quad \left. + \int_0^{1} \left[\frac{\partial v}{\partial x}\right]_{\text{right}} \mathrm{d}y \, V_{\text{w,right}} \right\}. \end{aligned} \tag{3}$$

At steady state the energy balance is achieved, thus $Q_{\text{net}} = W_{\text{net}}$.

It should be emphasized that, for convenience, we have absorbed all the dimensional properties on the work side of the energy equation. Therefore, Q_{net} and W_{net} definitions are representative of net heat transfer and net work with a proportionality coefficient which appears through non-dimensionalization of (1). The individual local quantities are now calculated as

$$Q_{\text{left}}(y) = -\left[\frac{\partial T}{\partial x}\right]_{\text{left}} \tag{4}$$

and similarly for $Q_{\text{right}}(y)$, $Q_{\text{top}}(x)$ and $Q_{\text{bottom}}(x)$. Also

$$W_{\text{left}}(y) = \left[\frac{\partial v}{\partial x}\right]_{\text{left}} (\gamma - 1) Pr M_{\text{f}}^2 V_{\text{w,left}} \tag{5}$$

and similarly for $W_{\text{right}}(y)$. For net wall values, we have

$$Q_{\text{net,left}} = \int_0^{1} Q_{\text{left}} \, \mathrm{d}y, \quad W_{\text{net,left}} = \int_0^{1} W_{\text{left}} \, \mathrm{d}y \tag{6}$$

and similarly for $Q_{\text{net,right}}$, $Q_{\text{net,top}}$, $Q_{\text{net,bottom}}$, and $W_{\text{net,right}}$.

Fig. 3 shows the temporal variation of net energy, i.e. $Q_{\text{net}} - W_{\text{net}}$, for different cases. The curves trail-off to zero which shows that equilibrium is achieved at steady state for all the cases. Cases IV and V show interesting peaks which are more pronounced for case V. An explanation for such behaviors can be given by studying the distribution of heat transfer and work done at the walls during this time period (i.e. 32–45 time units). This is discussed in the next section. Refer to Fig. 2 for comparisons of flow patterns at these times.

3.3. Distribution of heat transfer and work through the walls

This study is conducted for case V because the flow evolution for this case shows partially merged larger vortices (like cases II–IV) and a two-vortex stage with partially merged smaller vortices in the center (like case VI). Thus, a study of this case will be helpful in understanding all

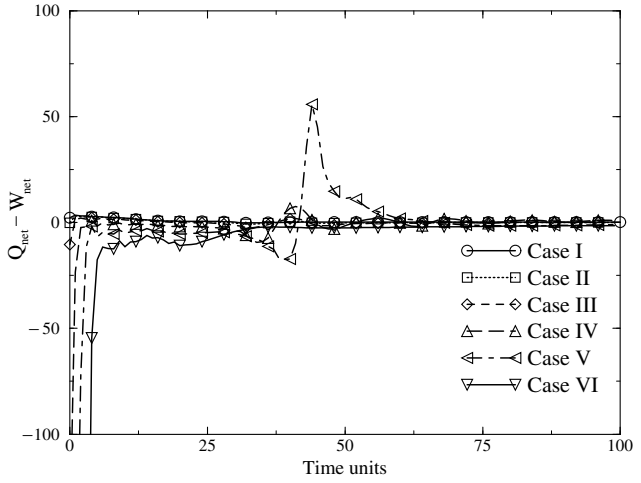

Fig. 3. Energy balance for all cases.

the cases. Heat transfer and work on various walls for this case are shown in Fig. 4 at four different times. It should be emphasized that distributions of heat transfer and work on the left and right walls show the smoothing of velocity and temperature boundary conditions near the corner in order to overcome the discontinuity at the corners.

After 32 time units, the smaller vortex on the (hot) right wall side starts gaining strength as discussed earlier. At 39 time units, the works done at the left and the right walls (Fig. 4(e) and (f)) do not change much as compared to the same at 32 time units. When the same comparison is made for the amount of heat transfer at the right wall (Fig. 4(d)), it is seen that the amount of heat transfer increases at 39 time units as compared to that at 32 time units because of the two newly formed counter-rotating vortices on the right wall side (see Fig. 2). Owing to the high heat transfer at the right wall at this time, the fluid coming towards the left wall is hotter and, therefore, the temperature gradient near the left wall is higher which means the heat transfer at the left wall is higher at 39 time units (Fig. 4(c)). This heat transfer by the two vortices also makes the heat transfer at the right side of the top wall (Fig. 4(b)) and the bottom wall (Fig. 4(a)) higher at this time. Note that the two counter-rotating vortices near the right wall at this time are the smaller vortex on the upper right corner which has by now gained strength, and the small portion of the larger partially merged elliptical vortex on the bottom right corner. Referring to the previous section, the above discussion explains the fact that the curve for case V in Fig. 3 shows that approximately at 32 time units, Q_{net} starts decreasing as compared to W_{net} and the curve reaches a negative peak at about 39 time units.

After 39 time units, the asymmetric elliptical vortex separates into two vortices, because of the upper right corner vortex trying to become circular. This gives the upper smaller vortex more space near the upper center portion of the cavity where it grows. The two counter-rotating vortices therefore move towards the upper right side of the cavity, and also gain a higher velocity. Thus, this area near $y = 0.6$ acts as a jet on the right moving wall. A character-

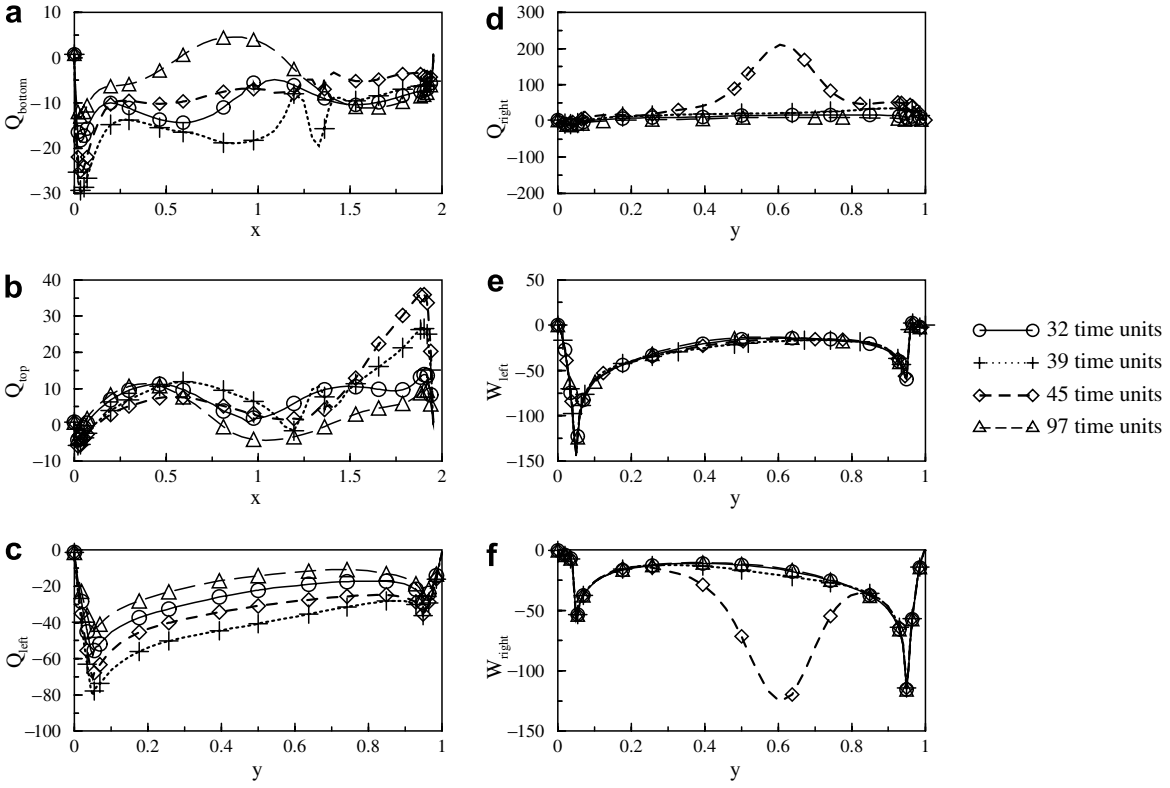

Fig. 4. Distribution of heat transfer and work at the walls during flow evolution for case V.

istic feature of this flow arrangement is an intensive heat transfer between the fluid and the wall. The vortex structures originate from the shear layer, which is in front of the virtual nozzle-like area, where the fast jet fluid mixes with the bulk fluid very near the wall. The vortices roll-up, are convected downstream, and interact with the wall. This interaction is represented by ejections of the boundary layer fluid and its replacement by the bulk fluid. The ejection and replacement process increases the velocity gradients and heat transfer rate on the wall. High velocity gradients result in high amount of work at this location. Fig. 4(d) and (f) shows the heat transfer and work done at the right wall. The area near $y = 0.6$ in this graph shows peaks in work and heat transfer for 45 time units. As the jet is now impinging towards the top side of the right wall, the heat transfer at the top wall increases near the right side and the bottom wall heat transfer decreases as compared to before.

Referring back to the previous section, the curve for case V in Fig. 3 at 45 time units, shows a positive peak and then starts decreasing and reaches equilibrium later. After 45 time units, the vortex separated from the elliptical vortex structure, occupies most of the space adjacent to the right wall due to which most of the heat transfer from the right wall is to this vortex. Meanwhile, the other two smaller vortices try to become circular and larger and in the process, combine. At steady state, the heat transfer is less on all the four walls compared to 45 time unit flow stage and the work done at the two moving walls also stabilizes because the jet action has now vanished.

The temporal changes in the net works done at the left and right walls and the net heat transfers at all the four walls are presented in Fig. 5(a)–(f) for cases I–VI, respectively. The work done at the walls is negative for all cases because work is done on the system by moving the walls. When the initial temperature and boundary temperatures are equal, i.e. in case I, the heat is generated in the system due to viscous friction between the layers of fluid. Therefore, there is heat transfer from the system through all the walls. These values therefore are negative in Fig. 5(a). For cases with sufficient differences in temperatures at the moving walls, the (cold) left wall is expected to transfer heat out of the system (negative) and the (hot) right wall is expected to transfer heat into the system (positive). For ±5% temperature difference case, i.e. case II shown in Fig. 5(b), there is still a heat transfer out of the system (negative) at the right (hot) wall. This suggests that the heat produced by viscous dissipation is larger than the heat transferred out of the system through the other three walls. For a higher percentage difference of temperatures than ±5%, i.e. cases III–VI, the heat transfer from the right (hot) wall is into the system (positive) and vice versa for the left wall.

The coupled effect of the two moving walls, gives a clockwise motion to the fluid flow patterns inside the cavity. Therefore, for cases with unequal temperature boundary

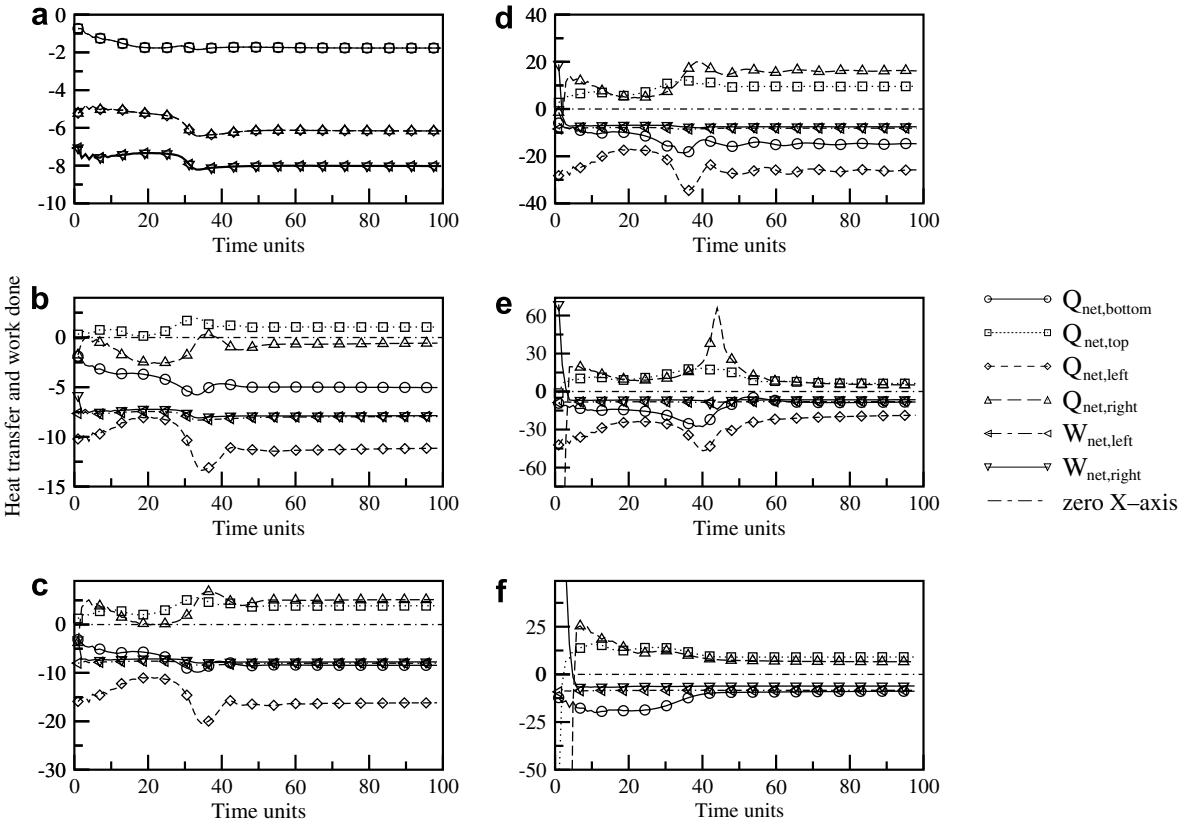

Fig. 5. Temporal evolution of total heat transfer and total work at the walls. (a)–(f) represent cases I–VI, respectively.

conditions, the fluid near the bottom wall carries heat from the (hot) right wall and vice versa for the top wall. As a result, there is heat transfer into the system (positive) at the top wall and heat transfer out of the system (negative) at the bottom wall (see Fig. 5(b)–(f) for cases II–VI). For case I, the left and right walls transfer more heat compared to the top and bottom walls. This is because of the motion of the moving walls which effectively brings more surface area in contact with the fluid in the same amount of time as compared to the stationary walls. For cases II–VI, where the temperatures of the moving walls are different from the initial temperature, the temperature gradient at the moving walls is higher than the stationary walls. Thus, the heat transfer at the moving walls is higher. Also, for all the cases the velocity gradient and, therefore, the viscous dissipation near the moving walls is higher compared to the stationary walls. Therefore, heat generation and heat transfer are higher near the moving walls.

As the temperature difference is increased, the net heat transfers at the left and the right walls increase. However, these values are higher for case IV (Fig. 5(d)) than for cases V and VI (Fig. 5(e) and (f)) at steady state. This is due to the velocity field near the right wall. The two vortices formed near the (hot) right wall in case IV, serve as a jet and give rise to an ejection-replacement process near the right wall. Due to the higher rate of mass transfer, there is a higher heat transfer. This situation is not present in cases V and VI at steady state. Therefore, the heat transfer near the right wall for case IV is higher as compared to cases V and VI. Also, in case IV, the asymmetrical elliptical vortex, a part of which is one of the vortices contributing to the impinging jet action, transfers heat better than the two vortices in cases V and VI at steady state. Thus, heat transfer at the left wall for case IV is also higher than heat transfer at the left wall for cases V and VI at the final stage.

Fig. 6 presents the steady state distribution of local heat transfer and local work done at all the walls for different cases. The heat transfers and the works at the left and right walls reflect the smoothing of velocity and temperature boundary conditions near the corner in order to overcome the discontinuity at these locations. For unequal wall temperature cases II–IV, heat transfer at the right wall is altered by the jet-like action on the moving (hot) right wall. The higher the temperature of the right wall, the

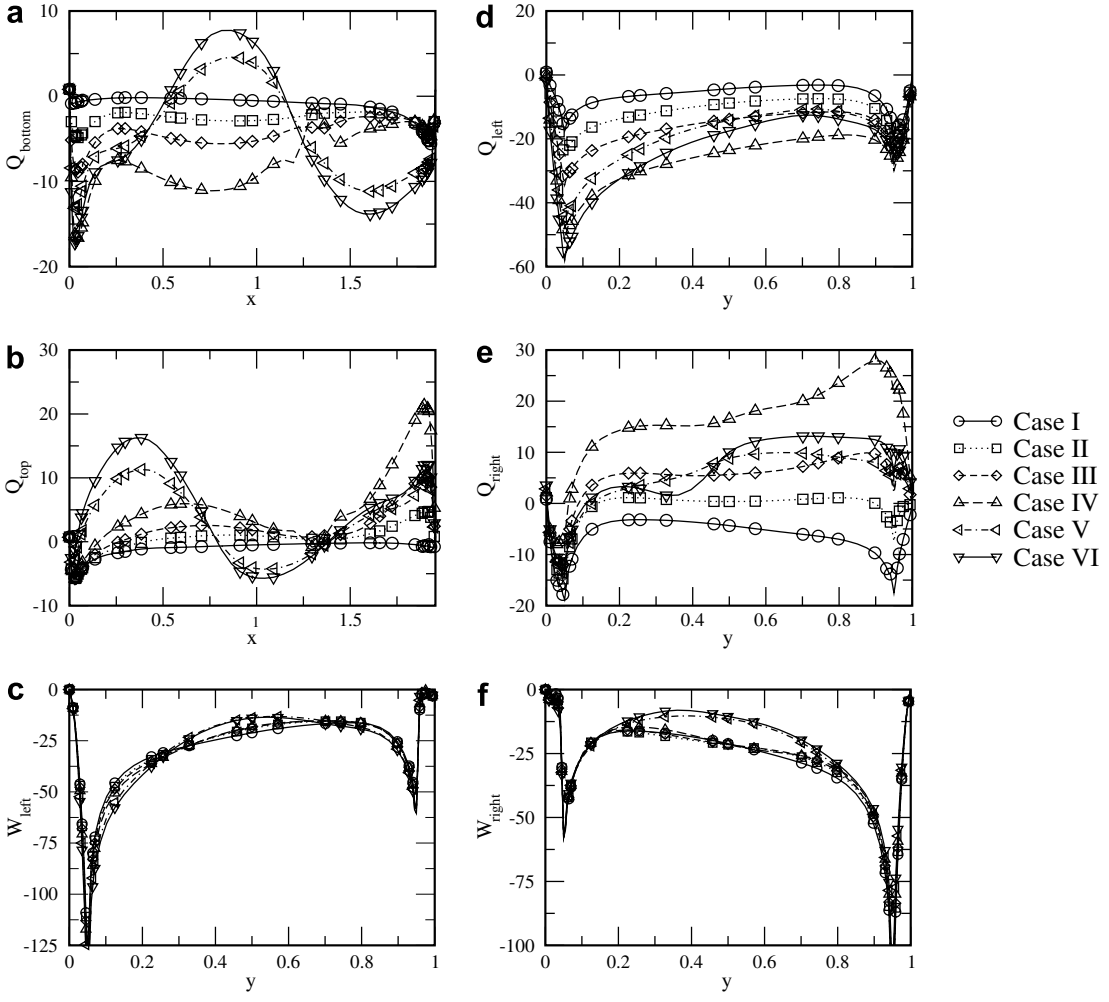

Fig. 6. Distribution of heat transfer and work at the walls at steady state for cases I–VI.

faster is the ejection (from the jet-like fluid flow) and replacement process near this wall, and therefore, case IV shows the maximum heat transfer. By contrast, in cases V and VI, i.e. for ±30% and ±40% difference in temperatures at the moving walls, the steady state is a two-vortex stage. Because of this, the heat transfer reduces in these cases as compared to case IV.

For unequal wall temperature cases II–IV, heat transfer at the left wall also increases as the difference between temperatures of the walls increases. This is because, the elliptical vortex, which extends from the left to the right wall, transfers hot fluid from the (hot) right side to the left side of the cavity which is cold. Thus, the temperature gradient increases on the left side. Cases V and VI, at steady state show a two-vortex flow pattern. Thus, the heat transfer is less from the right wall to the left side and therefore, the temperature gradient on the left side is lower which results in less heat transfer at the left walls in these cases as compared to case IV.

We now draw our attention to heat transfer at the top and bottom walls for cases V and VI. The steady state flow pattern for these cases is a two-vortex stage with two smaller vortices in the center. Now, the coupled effect of motion of the left and right walls in clockwise direction makes both the larger vortices (one on the cold (left) side and another on the hot (right) side), rotate in a clockwise direction. Thus, the heat gained by the vortex on the right wall is lost at the bottom wall on the right side. Vice versa is the case at the left vortex side. The heat transfer curves, therefore, show large fluctuations at these locations.

The works done at the walls do not show much difference in cases I–IV but decrease for cases V and VI. The reason can be explained by examining the velocity vectors (not shown here) near the right wall at steady state for cases I–VI. The velocity vectors for cases I–IV do not show much difference, but when the boundary layers of cases I–IV are compared with those of cases V and VI, it is observed that the velocity gradient at the right wall for cases V and VI is smaller as compared to that in cases I–IV and, therefore, the work done is lower in cases V and VI.

3.4. Practical observations

In the roll coating process, a coating fluid flows with a very low velocity into a narrow gap between two rotating cylinders, the surfaces of which move in opposite directions. The two rolls with large radii represent two moving walls. The liquid passes through the gap and splits downstream into two uniform thin films, each coating one of the rolls. The requirement is that the layer of liquid should be thin, continuous, uniform in thickness and smooth. These qualities in a film of fluid cannot be obtained at high speed flows because of instabilities generated in a single vortex. Flow instabilities and asymmetry is seen to occur at steady state in cases I–III. However, the requirements can be met if the percentage temperature difference is kept higher than 20%, i.e. cases V and VI, where the final stage is a two-vortex pattern. The work done at the left and right walls in cases V and VI is also less compared to other cases.

Variants of the two-sided lid-driven cavity have been employed to study drying processes [9]. This application is useful for drying paper during recycling by two counter-rotating cylinders. It is also used for removing solvents from a thin liquid film on a moving porous surface. A dryer can be modeled as a shallow cavity with two facing walls moving tangentially, filled with a mixture of gas and solvent vapor. Heat is supplied to one moving wall in order to stimulate the evaporation of the liquid solvent. The other wall is cooled so that the solvent vapor in the cavity should condense on it [9]. In the previous section, we saw that maximum heat transfer is obtained at the left and the right walls for case IV which has $T_{w,right} = 1.2T_i$ and $T_{w,left} = 0.8T_i$. Giving a higher temperature difference would result in less heat transfer at the two walls. Thus, case IV would be the optimum case for such a model wherein, maximum heat transfer is obtained with optimum work done on the two moving walls.

4. Conclusions

The viscous, compressible flow in a two-dimensional lid-driven cavity with unequal moving walls temperatures is studied numerically using a Chebyshev multi-domain spectral element method. An asymmetry in temperature boundary conditions of the two moving walls leads to an asymmetric flow pattern at the steady state, however, a very high asymmetry ($\geqslant \pm 30\%$) results in a symmetric flow pattern at steady state. When unequal temperature boundary conditions are employed on the two moving walls, high temperature gradients arise. The higher is the temperature difference between the two moving walls, the harder and therefore later is the combination of the two vortices into a single vortex owing to asymmetry. The flow in a cavity with low aspect ratio, with unequal temperatures at the moving walls, behaves like the flow in a cavity with higher aspect ratio and same temperatures of the moving walls. There is an intensive heat transfer between the fluid and the hot wall when, because of a temperature difference between the two moving walls, a jet-like flow pattern is formed on the hot wall. When the boundary temperatures are equal, the heat is generated in the system due to viscous friction between the layers of fluid, and there is heat transfer from the system through all the walls. For cases with sufficient differences in temperatures at the moving walls, the cold wall transfers heat out of the system and the hot wall transfers heat into the system. There is heat transfer into the system at the top wall and heat transfer out of the system at the bottom wall. For all cases with unequal temperature boundary conditions, the moving walls transfer more heat compared to the stationary walls.

For an aspect ratio of 1.955, Reynolds number of 700 and Mach number of 0.4, when the moving wall temperatures are ±20% different than the initial temperature, i.e. $T_{w,right} = 1.2T_i$ and $T_{w,left} = 0.8T_i$, heat transfer is the

highest. The work done though does not show much difference. Giving a higher temperature difference would result in less heat transfer at the two walls. Thus, ±20% would be the optimum temperature difference for such a model wherein, maximum heat transfer is obtained with optimum work done at the two moving walls. This may be considered as the optimum temperature difference for drying processes under similar configuration. The requirements for coating a roll with uniform, smooth and thin film may be met if the percentage temperature difference is kept higher than 20%, where the final stage is a two-vortex pattern.

Acknowledgements

This work was supported in part by the US Office of Naval Research and the National Science Foundation.

References

[1] P. Shah, B. Rovagnati, F. Mashayek, G.B. Jacobs, Subsonic compressible flow in two-sided lid-driven cavity. Part I: Equal walls temperatures, Int. J. Heat Mass Transfer, in press, doi:10.1016/j.ijheatmasstransfer.2007.02.028.

[2] O. Aydin, Aiding and opposing mechanisms of mixed convection in a shear and buoyancy driven cavity, Int. Commun. Heat Mass transfer 26 (1999) 1019–1028.

[3] S.K. Mahapatra, A. Nanda, P. Sarkar, Interaction of mixed convection in two-sided lid driven differentially heated square enclosure with radiation in presence of participating medium, Heat Mass Transfer 42 (2006) 739–757.

[4] P. Gandhi, Numerical investigation of compressible flow in two-sided lid-driven cavity, MS Thesis, University of Illinois at Chicago, Chicago, IL, 2003.

[5] D.A. Kopriva, A staggered-grid multidomain spectral method for the compressible Navier–Stokes equations, J. Comput. Phys. 244 (1998) 142–158.

[6] G.B. Jacobs, D.A. Kopriva, F. Mashayek, A comparison of outflow boundary conditions for the multidomain staggered-grid spectral method, Numer. Heat Transfer, Part B 44 (3) (2003) 225–251.

[7] G.B. Jacobs, Numerical simulation of two-phase turbulent compressible flows with a multidomain spectral method, Ph.D. Thesis, University of Illinois at Chicago, Chicago, IL, 2003.

[8] H. Schlichting, Boundary-Layer Theory, seventh ed., McGraw-Hill Book Co., 1979.

[9] N. Alleborn, H. Raszillier, F. Durst, Lid-driven cavity with heat and mass transport, Int. J. Heat Mass Transfer 42 (1999) 833.